Systemic translocation of *Staphylococcus aureus* promotes autoimmunity: implications in autoantibody-mediated poor immune reconstitution from antiretroviral therapy in HIV

Short title: Autoimmunity in HIV immunopathogenesis

Da Cheng[1], Zhenwu Luo[1], Wangbin Ning[1], Sonya L. Heath[2], Magnus Gisslen[3,4,5], Richard W Price[6], Ruth Adekunle[7,8], Tabinda Salman[1], Douglas Johnson[1], John E McKinnon[7,8], Lishomwa C. Ndhlovu[9], Reafa Hossain[10], Wenhui Hu[10], Wei Jiang[1,7,8*]
(ORCiD 0000- 0002-1374-053X)

[1]Department of Pharmacology and Immunology, Medical University of South Carolina, Charleston, SC, 29425, USA.
[2]Division of Infectious Diseases, Department of Medicine, University of Alabama at Birmingham, Birmingham, AL, 35294, USA.
[3]Department of Infectious Diseases, Institute of Biomedicine, Sahlgrenska Academy, University of Gothenburg, 41645, Gothenburg, Sweden
[4]Department of Infectious Diseases, Sahlgrenska University Hospital, Region Västra Götaland, Gothenburg, Sweden
[5]Public Health Agency of Sweden, Solna, Sweden
[6]Department of Neurology, University of California, San Francisco, San Francisco General Hospital, San Francisco, CA, 94110, USA
[7]Department of Medicine, Division of Infectious Diseases, Medical University of South Carolina, Charleston, SC, 29425, USA.
[8]Ralph H. Johnson VA Medical Center, Charleston, SC, USA
[9]Department of Medicine, Division of Infectious Diseases, Weill Cornell Medicine, New York, NY, 10021, USA
[10]Department of Anatomy and Neurobiology, Virginia Commonwealth University, Richmond, Virginia, 23298-0709, USA

*Corresponding author: Wei Jiang, 173 Ashley Ave. Charleston, SC, 29425, email: jianw@musc.edu

Abstract

Background: In 2017, our group first demonstrated that autoimmunity contributes to HIV pathogenesis, even without autoimmune disease. This concept is now broadly recognized, exemplified by the role of autoimmunity in severe COVID-19. In people with HIV (PWH) on suppressive ART, anti-CD4 autoantibodies may impair CD4+ T cell recovery, though the mechanisms driving their production remain unclear. Building on evidence from our group and others that *Staphylococcus aureus* and its peptidoglycan (PGN) promote autoimmunity, we investigated their contribution to anti-CD4 IgG in HIV.

Methods: Plasma from 32 ART-naive PWH, 53 ART-treated PWH, and 32 HIV-negative controls was analyzed for IgG autoantibodies and markers of *S. aureus* translocation using protein array, ELISA, and microarray. EcoHIV mice were injected intraperitoneally with saline, *S. aureus* PGN, or *Bacillus subtilis* PGN. PGN structures were compared by mass spectrometry.

Results: Among 87 autoantibodies, 40% were elevated in ART-naive PWH and largely normalized by ART; however, anti-CD4 IgGs remained elevated in PWH on ART. Anti-CD4 IgG levels inversely correlated with CD4+ T cell counts in ART-treated PWH and positively with *S. aureus* translocation. In mice, *S. aureus* PGN induced anti-CD4 IgGs, reduced gut CD4+ T cells, and promoted surface IgG binding and apoptosis in CD4+ T cells.

Conclusion: *S. aureus* and its PGN translocation may drive anti-CD4 autoimmunity and hinder immune recovery in PWH on suppressive ART, highlighting *S. aureus* colonization as a therapeutic target and supporting the development of competitive probiotic interventions such as *Bacillus subtilis*.

Keywords: HIV, autoimmunity, anti-CD4 autoantibodies, failed immune reconstitution, microbiome, *Staphylococcus aureus*

Introduction

Recent studies, including ours, show that autoimmunity contributes to pathogenesis in infectious diseases without clinical autoimmune conditions (1). About 20% of PWH on ART fail to restore CD4+ T cell counts despite viral suppression, increasing comorbidity and mortality risks (2). We demonstrated that anti-CD4 autoantibodies drive CD4+ T cell death via ADCC, contributing to poor immune reconstitution post-ART (3), a finding supported by other researchers (4), though outcomes vary (5). The mechanisms driving anti-CD4 IgG production in HIV remain unclear.

Our prior work (6) demonstrated that S. aureus PGN induces pathogenic autoantibodies and kidney injury in SLE. Intraperitoneal injection of heat-killed S. aureus or its PGN elicited autoantibody responses in both C57BL/6J and autoimmune-prone mice (6, 7). As a major antigenic cell wall component, PGN exerts distinct immune effects depending on its bacterial source (8). Because S. aureus colonization is more frequent in PWH (9), we examined links between autoantibodies and CD4+ T cell counts and tested the role of S. aureus PGN in anti-CD4 IgG production. Our findings show that S. aureus PGN promotes anti-CD4 IgG generation, leading to CD4+ T cell loss and impaired immune recovery in PWH on suppressive ART.

Results

Autoantibody landscape and the unique characteristics of anti-CD4 IgGs

Among the 87 autoantibody IgGs (autoIgGs) in HIV+/ART+, 35 autoIgGs (40%) were elevated, 3 were reduced, and the rest were similar to controls (Figure 1A). ART normalized most autoIgGs, but anti-CD4 and anti-prothrombin IgGs remained elevated in HIV+/ART+ (Figure 1A-1B). Anti-CD8 IgG was lower in HIV+/ART-naive versus controls (Figure 1C). Plasma anti-CD4 IgG levels inversely correlated with CD4+ T cell counts in HIV+/ART+ only (Figure 1D). Anti-CD4 IgM and IgA levels were comparable across groups. In HIV+/ART+, anti-CD4 IgG1 and IgG3, but not IgG2 or IgG4, were elevated (Figure S1A-S1B) (3, 10). IgG1 and IgG3 in humans support ADCC (11, 12). In addition, plasma levels of anti-prothrombin IgG were directly correlated with anti-CD4 IgGs ($r = 0.22$, $P = 0.01$), but not correlated with CD4+ T cell counts ($r = -0.16$, $P = 0.22$).

Elevated anti-CD4 IgG levels are associated with plasma levels of *S. aureus* translocation in PWH on suppressive ART

Our previous study in systemic lupus erythematosus (SLE) demonstrated that *Staphylococcus aureus* contributes to the production of pathogenic lupus-associated anti–double-stranded DNA IgG antibodies and to kidney damage (6). Based on these findings, we evaluated the potential role of *S. aureus* in the generation of anti-CD4

autoantibodies in HIV infection. To assess systemic exposure to *S. aureus*, we measured plasma IgG levels against *S. aureus* antigens as a surrogate of bacterial translocation. We found that plasma IgG levels against *S. aureus* antigens were positively correlated with anti-CD4 IgG levels in HIV+/ART+ individuals. (Figure 2A-2B).

S. aureus PGN induced anti-CD4 IgG production in EcoHIV mice

EcoHIV mouse study design is shown in Figure 3A and infection was verified by qPCR (Figure S2). S. aureus PGN increased serum anti-CD4 IgG without affecting total IgG (Figure 3B), indicating limited polyclonal B cell activation. In mice, IgG2a and IgG2b mediate ADCC (13), and S. aureus PGN selectively increased anti-CD4 IgG2b and IgG3 (Figure 3C). By contrast, B. subtilis PGN, a probiotic (14), did not induce anti-CD4 IgG (Figure 3B–3C).

S. aureus PGN reduced gut CD4+ T cells through apoptosis of IgG-bound CD4+ T cells in EcoHIV mice

Furthermore, S. aureus PGN decreased CD3+CD4+ T cells (Figure 3D) and increased surface-bound autoIgG on CD4+ T cells in the gut, but not in blood or spleen (Figure 4A–4D). IgG+CD4+ T cells were highly apoptotic at all sites, in contrast to IgG–CD4+ T cells (Figure 4E-4G). CD4−CD3+ T cell frequencies were unaffected, with minimal IgG binding (Figure S3). In vitro, S. aureus PGN did not

directly induce gut CD4+ T cell apoptosis (Figure S4). These results indicate that S. aureus PGN indirectly drives gut CD4+ T cell apoptosis through autoIgG binding.

S. aureus PGN drives class switch DNA recombination (CSR) via TLR2 in vitro.

Both native and heat-inactivated S. aureus PGN promoted CSR through TLR2, unlike B. subtilis PGN (Figures 5A–5B, S5A–S5C, S6). Notably, B. subtilis PGN induced stronger TLR2 signaling than S. aureus PGN (Figure S5D), suggesting that S. aureus PGN–mediated CSR involves additional mechanisms beyond TLR2 activation.

PGN structural analysis

S. aureus PGN (~18 disaccharide units) contains muramic acid (Mur) and the amino acids Lys, Ala, Gly, and Glu, with a molar ratio of 1.4 Ala: 2.9 Gly: 1.0 Glu: 1.1 Lys (GC/MS). In contrast, B. subtilis PGN (80–250 disaccharide units) contains Mur, Dpm, Ala, and Glu, with a molar ratio of 1.0 Ala: 1.0 Glu: 0.8 Dpm, and includes meso-Dpm and D-Glu enantiomers. Structurally, S. aureus PGN is classified as A3α (L-Lys–Gly_{5-6}, L-Lys–Gly_3), while B. subtilis PGN is A1γ (meso-Dpm–direct), accounting for their distinct immunomodulatory properties.

Discussion

Autoimmunity contributes to infectious disease pathogenesis, even in the absence of clinical autoimmune disease (1). We first reported anti-CD4 IgG autoimmunity in HIV in 2017, linking it to CD4+ T cell depletion and poor immune recovery post-ART (3), a finding later supported by others (15, 16). Here, we show that S. aureus translocation drives anti-CD4 IgG production, potentially explaining higher CD4+ T cell recovery failure in African PWH with prevalent S. aureus colonization (17).

Anti-CD4 IgG was first described in the pre-ART era (18), but its pathogenicity remained unclear until our 2017 study demonstrated its role in poor CD4+ T cell recovery post-ART (3). Recent studies show that anti-CD4 IgG levels rise during untreated HIV infection, decline with ART, yet persist in a subset of PWH on ART; an inverse correlation with CD4+ T cell counts was observed at 48 and 96 weeks post-ART, but not before ART or at 24 weeks (10), while other reports found no association after prolonged ART (5). Low-affinity, non-cytotoxic natural autoantibodies may emerge from chronic inflammation (19), whereas pathogenic autoantibodies require disordered somatic hypermutation and CSR over time. Unlike pre-ART anti-CD4 IgGs, which are non-cytotoxic natural autoantibodies likely induced by viremia and inflammation, pathogenic anti-CD4 IgGs in PWH on ART mediate ADCC and develop post-ART (15, 20-22). Anti-prothrombin IgG (aPT IgG) is

an antiphospholipid antibody directed against prothrombin; our study reveals that plasma levels of anti-prothrombin IgG were directly correlated with anti-CD4 IgG levels, but not with CD4+ T cell counts, suggesting that these two autoantibodies may be generated through a similar mechanism and anti-prothrombin IgG does not contribute to CD4+ T cell counts. Previous studies (23, 24) have shown increased levels of anti-prothrombin IgG in HIV-infected, predominantly ART-untreated individuals; however, these antibodies were typically transient and not strongly associated with thrombotic events or overt antiphospholipid syndrome.

S. aureus colonization and antigen translocation alone may not trigger pathogenic autoantibody production without a compromised barrier, immune perturbations, or genetic predisposition to autoimmunity. Unlike autoantibodies in autoimmune diseases, pathogenic anti-CD4 IgG in PWH on suppressive ART may arise from: 1) elevated apoptotic CD4+ T cells increasing CD4 self-antigen in lymph nodes (25); 2) persistent viral protein release, including HIV gp120, enhancing CD4 binding to anti-CD4 IgG and promoting its production (26); 3) the absence of autoimmune-prone genetic backgrounds in most PWH differentiates these responses from classical autoimmune diseases.

CD4+ T cell apoptosis was detected only in mesenteric lymph nodes, not in the spleen or blood, after S. aureus PGN administration. Although IgG+CD4+ T cells

exhibited higher levels of apoptosis than IgG−CD4+ T cells across all sites (Figure 4E-4G), increased IgG surface binding on CD4+ T cells following *S. aureus* PGN intraperitoneal injection was observed only in mesenteric lymph nodes, and not in the spleen or blood (Figure 4B-4D). The site-specific effects likely reflect differences in local exposure to SA-PGN following intraperitoneal administration. Mesenteric lymph nodes are expected to encounter higher concentrations of SA-PGN than the spleen or peripheral blood. Since SIV/HIV infection initiates CD4+ T cell loss in the gut during acute infection and progresses to peripheral depletion in chronic stages (27), we hypothesize that prolonged exposure to S. aureus PGN (e.g., 1 year) may also deplete peripheral CD4+ T cells. Importantly, mesenteric CD4+ T cell death was not induced by PGN directly in vitro, suggesting an indirect mechanism via autoIgG binding and cell apoptosis. The mechanisms driving S. aureus PGN-mediated gut autoIgG production and CD4+ T cell decline require further studies.

Previous studies reveal that bacterial lipoteichoic acid (LTA), a TLR2 ligand, primarily induces TLR2-dependent pro-inflammatory cytokines rather than autoantibodies (6, 28). Generally, TLR2 signaling in B cells more often supports cytokine secretion, activation marker upregulation, or differentiation than direct mitogenesis, comparable to strong mitogens such as CpG (TLR9) or anti-IgM (29). In addition, the downstream pathways and outcomes of TLR2 activation can differ in cytokine production and proliferation. S. aureus PGN exhibited structural differences compared with B. subtilis

PGN. An additional mechanism may account for S. aureus PGN-mediated B cell CSR, which warrants further investigation.

The limitations of this study are: 1) there is no figure reported by the PGN structure analysis from the company (Creative Proteomics, Shirley, NY, USA); 2) the potential contamination of protein A or LTA in S. aureus PGN. Nonetheless, several lines of evidence support PGN as a driver of autoantibody production: (1) a TLR2 inhibitor blocked PGN effects; (2) PGN, but not the other Gram+ bacterial products, is detectable in human circulation without a clinical bacterial infection (8); (3) S. aureus protein A and enterotoxin B reduce lupus autoimmunity in mice (30, 31); and (5) LTA, a TLR2 ligand, primarily induces pro-inflammatory cytokines rather than autoantibodies (6, 28).

Currently, no treatment is available for improving CD4+ T cell recovery in PWH on suppressive ART. Up to 20% of PWH on ART fail to restore peripheral CD4+ T cell counts to the levels of healthy controls; increased morbidity and mortality have been demonstrated in these patients, which is the main challenge in the HIV clinic. This study reveals that *S. aureus* and its PGN translocation may drive anti-CD4 autoimmunity and hinder immune recovery in PWH on suppressive ART, highlighting *S. aureus* colonization as a therapeutic target and supporting the development of competitive probiotic interventions such as *Bacillus subtilis* (32).

Materials and methods

Human subjects

This study enrolled 32 controls (without HIV), 32 HIV+/ART-naïve, and 53 HIV+/ART+ individuals (>2 years undetectable plasma HIV-1 RNA) from Sahlgrenska University Hospital (Gothenburg, Sweden), San Francisco General Hospital (San Francisco, CA, USA), Ralph H. Johnson Veteran Health Care System (RHJ VAHCS, SC, USA), and the Medical University of South Carolina (MUSC, SC, USA). The local institutional review board approved the study. Demographics and clinical details are provided in Table 1. PWH were divided into low and high anti-CD4 IgG subgroups using a 35 ng/ml cutoff, based on the 95th percentile in controls.

Autoantigen protein array, B-cell gene profiles, and plasma levels of anti-CD4 autoantibodies

We reported the methods of protein array containing 87 self-antigens, B cell gene microarray, and plasma anti-CD4 autoantibody levels (3, 7).

Plasma *S. aureus* antigen translocation

S. aureus lysate was prepared using the BugBuster Master Mix and coated onto high-binding plates (Sino Biological, Wayne, PA) at 2 µg/100 µL/well. The plate was blocked with 3% BSA and added with diluted plasma samples (1:4000 for IgA,

1:400000 for IgG). Detection was performed using horseradish peroxidase-labeled anti-human IgG and IgA.

Bacterial PGN structural analysis

PGNs from *S. aureus* (ATCC, 6538P) and *B. subtilis* (NR-607, BEI, Manassas, VA) were separated with an Agilent HPLC system and analyzed using mass spectrometry (Creative Proteomics, Shirley, NY, USA).

Mice Experiment

Mouse study design was shown in Figure 3A. EcoHIV plasmid was obtained from Dr. Hu (Virginia Commonwealth University) (33). Six-week-old female C57BL/6J mice (Jackson Laboratory, Bar Harbor, ME) received mixed antibiotics (Gibco™, 1 mg/mL) in drinking water for 3 days and a 2-day break. Mice were injected i.p. with EcoHIV (50 μL, 3.45 × 10^8 IU/mL; n = 6/group), followed by i.p. of PBS, S. aureus PGN, or B. subtilis PGN (InvivoGen, San Diego, CA) twice weekly for 12 weeks. Whole blood was drawn via the tail vein method from EcoHIV-injected mice under aseptic conditions. To verify ecoHIV infection, the blood was used to isolate DNA via the Quick-DNA/RNA Miniprep Plus Kit (Zymo; Irvine, CA, Cat # D7003). The standard curve was generated from viral titer and threshold cycles using the ABM qPCR lentivirus titer kit (LV900). qPCR for HIV-LTR was performed for the unknown and standard samples via QuantaBio PerfecTa Toughmix (QuantaBio, Beverly, MA),

supplemented with the following primers and a probe: LTRF, 5'-CTGGCTAATTAGGGAACCCACTG-3'; LTRR, 5'-GGACTAAACGGATCTGAGGGATCTC-3'; and the LTRP, 5'-(FAM)-TTACCAGAGTCACACAACAGACGGGCA-(MGBNFQ)-3'. The thermal program used was 3 min at 55°C, 10 min at 95°C, and 40 cycles of 15 sec at 95°C and 1 min at 60°C. qPCR was performed at the Bio-Rad CFX96 qPCR instrument (Bio-Rad Laboratories, Hercules, CA), and data analysis was done with the built-in Bio-Rad software. The number of proviral copies in the unknown sample is the number of the total number of copies minus the number of copies in the control reaction. All samples were run in triplicate.

Mouse serum anti-CD4 IgG levels

Serum anti-CD4 IgG was detected using recombinant mouse CD4 protein (1 μg/100 μL/well) and horseradish peroxidase-labeled anti-mouse IgG or its subclasses.

B cell class switch DNA recombination (CSR)

B cells, isolated from spleens of 8-week-old mice (STEMCELL B Cell Negative Isolation Kit), were cultured with medium, S. aureus PGN, or B. subtilis PGN (10 μg/mL), ± anti-TLR2 or isotype IgG2a (100 ng/mL, InvivoGen), or positive controls (LPS from E. coli 055:B5 [3 μg/mL, InvivoGen] plus IFN-γ [50 ng/mL, BioLegend] or TGF-β1 [2 ng/mL, R&D Systems]). CSR was measured by proliferating IgG3 and

IgG2b B cell percentages using a BD FACSVerse™ Cell Analyzer after staining with anti-B220, anti-IgG2b, anti-IgG3, anti-CD138, and anti-IgM antibodies (BioLegend).

IgG surface binding on CD4+ T cells

Cells from blood, spleen, and mesenteric lymph nodes were stained with anti-CD3, anti-CD4, anti-IgG, Annexin V, and streptavidin, then analyzed on a BD FACSVerse™ flow cytometer using FlowJo software.

PGN-mediated TLR2 activity

TLR2 activity was detected using the HEK-Blue™ mTLR2 cells (InvivoGen) following the manufacturer's instruction.

Statistics

Data were analyzed using Student's t-test or Mann–Whitney test for two-group comparisons and one-way ANOVA for multiple groups. Associations were assessed by Spearman correlation. A P value < 0.05 was considered significant.

Authors' contributions

D.C. wrote the first version of the manuscript. D.C., Z.L., T.S., D.J., and W.N. performed experiments and analyzed data. M.G., R.W., S.H., and Z.L. recruited the study participants. D.C., Z.L., W.J., L.C.N., R.P., R.H., W. H., M.G., JEM, and R.A. were involved in critically revising the manuscript.

Conflicts of Interest

L.C.N. reports grants from the NIH and has received consulting fees from work as a scientific advisor for AbbVie, ViiV Healthcare, Ledidi AS, serves on the Board of CytoDyn and has financial interests in Ledidi AS all for work outside of the submitted work. All other authors declare no competing interests.

Acknowledgments

We thank John D. Dinolfo, Ph.D. (MUSC), for English language editing. This work was supported by the Ralph H. Johnson VA Health Care System I01CX002422 (Jiang) from the U.S. Department of Veterans Affairs; the VA Southeast Network 7 Research Development Award (Adekunle); NIH grants R01DA059854 (Jiang), R01DA059538 (Jiang), R01DA056876 (Hu), P30AI027767 (Saag/Health), R01NS094067 (Price), UL1TR001450, TL1TR002382 (Adekunle), and UL1TR002378 (Adekunle, TL1). The content is solely the responsibility of the authors and does not necessarily represent the official views of the NIH.

Availability of data and materials

Data are available.

Figure legends

Figure 1. HIV-associated IgG autoantibodies. (A) Z-scored plasma levels of 87 autoantibodies in controls (n = 32), untreated PWH (n = 32), and ART-suppressed PWH (n = 53). (B) Anti-CD4 and anti-prothrombin IgG. (C) Anti-CD8 IgG. (D) Correlation between anti-CD4 IgG and CD4+ T cell counts. ANOVA and Spearman correlation. Samples were analyzed for autoantibodies using a protein array and collected from four institutions: Sahlgrenska University Hospital, San Francisco General Hospital, RHJ VAHCS, and MUSC.

Figure 2. Association of S. aureus markers with anti-CD4 IgG in PWH on ART. (A) Correlation of plasma anti-CD4 IgG with anti-S. aureus IgG. (B) Elevated plasma anti-S. aureus IgG in HIV+/ART+. Spearman correlation and ANOVA. PWH were divided into low and high anti-CD4 IgG subgroups using a 35 ng/ml cutoff, based on the 95th percentile in controls. Samples from MUSC were analyzed for anti-CD4 IgG and anti-S. aureus IgG by ELISA.

Figure 3. S. aureus PGN induces anti-CD4 IgG and reduces gut CD4+ T cells in EcoHIV mice. C57BL/6J mice received i.p. PBS, S. aureus PGN, or B. subtilis PGN. (A) Mouse study design. (B–C) Serum anti-CD4 IgG, total IgG, and IgG subclasses. (D) Gating strategy and CD4+ T cell frequencies in the three sampling sites. Student's t-test and ANOVA.

Figure 4. S. aureus PGN increases apoptotic IgG+CD4+ T cells in gut-associated tissues. (A) Annexin V binding on IgG+ vs. IgG– CD4+ T cells. (B–D)

Frequencies of IgG+CD4+ T cells in mesenteric lymph nodes, spleen, and blood. (E–G) Annexin V binding on IgG+ vs. IgG– CD4+ T cells. Student's t-test and ANOVA.

Figure 5. S. aureus PGN induces CSR to IgG2b and IgG3 in vitro. Splenic B cells from naive C57BL/6J mice were cultured with medium, and PGNs (10 μg/mL) ± TLR2-mAb or isotype Ab (1 μg/mL) for 96 h. Percentages of proliferating IgG2b+ and IgG3+ B cells (%CFSE^{low}IgG2b/IgG3+ in B220+ cells) are shown (A–B). ANOVA.

Figure S1. **Elevated plasma anti-CD4 IgG1 and IgG3 subclasses in PWH on ART**. (A) The median plasma levels of anti-CD4 IgG, IgM, and IgA in controls (n = 15) and HIV+/ART+ subjects (n = 23). (B) The median plasma levels of anti-CD4 IgG subclasses (IgG1-IgG4) between the two groups. Mann-Whitney tests.

Figure S2. Confirmation of established EcoHIV infection in mice. The EcoHIV virus was verified by qPCR in blood samples collected one month after infection.

Figure S3. S. aureus PGN does not affect gut CD4−CD3+ T cells in vivo. (A) Gating strategy. (B) Percentages of CD4−CD3+ T cells among total CD3+ T cells and IgG+CD4−CD3+ T cells in mesenteric lymph nodes. ANOVA.

Figure S4. S. aureus PGN does not directly induce gut CD4+ T cell apoptosis in vitro. Lymphocytes from mesenteric lymph nodes were treated with S. aureus PGN (0.1–10 μg/mL) for 4 days. (A-B) Percentages of CD4+ T cells and Annexin V+CD4+ T cells. ANOVA.

Figure S5. PGN dose titration for CSR and TLR2 activity. (A–B) S. aureus PGN induced total (A) and proliferating (B) IgG2b+ B cells. (C) CSR induction by heat-inactivated vs. native S. aureus PGN. (D) mTLR2 reporter cell responses after 16 h treatment. ANOVA.

Figure S6. S. aureus PGN induces CSR in vitro. Splenic B cells from naive mice were cultured with PGN (10 μg/mL) for 96 h. Percentages of CD138+ IgG2b+ and IgG3+ plasmablasts (%CD138+CFSE^lowIgG2b/IgG3+ in B220+ cells) are shown (A–B). ANOVA.

Table 1 Clinical characteristics of study participants

	HIV-negative/Controls (n = 32)	HIV+/ART naive (n = 32)	HIV+/ART+ (n = 53)	P value (two HIV+ groups)

Age (years)	49 (34-58)	49 (35-55)	42 (36-52)	0.16
Sex ratio, male: female	21:11	22:10	37:16	0.92
CD4+ T cell counts	797 (554-916)	255 (98-490)	570 (456-724)	< 0.0001
Nadir CD4+ T cell counts		215 (97-490)	294 (164-464)	0.37
Duration of ART (years)			5.5 (4-6)	

ART, antiretroviral therapy; CD4+ T cell count (cells/μL)

Data are means (25th percentile, 75th percentile)

References

1. Bastard P, Rosen LB, Zhang Q, Michailidis E, Hoffmann HH, Zhang Y, Dorgham K, Philippot Q, Rosain J, Beziat V, Manry J, Shaw E, Haljasmagi L, Peterson P, Lorenzo L, Bizien L, Trouillet-Assant S, Dobbs K, de Jesus AA, Belot A, Kallaste A, Catherinot E, Tandjaoui-Lambiotte Y, Le Pen J, Kerner G, Bigio B, Seeleuthner Y, Yang R, Bolze A, Spaan AN, Delmonte OM, Abers MS, Aiuti A, Casari G, Lampasona V, Piemonti L, Ciceri F, Bilguvar K, Lifton RP, Vasse M, Smadja DM, Migaud M, Hadjadj J, Terrier B, Duffy D, Quintana-Murci L,

van de Beek D, Roussel L, Vinh DC, Tangye SG, et al. 2020. Autoantibodies against type I IFNs in patients with life-threatening COVID-19. Science 370.

2. Gazzola L, Tincati C, Bellistri GM, Monforte A, Marchetti G. 2009. The absence of CD4+ T cell count recovery despite receipt of virologically suppressive highly active antiretroviral therapy: clinical risk, immunological gaps, and therapeutic options. Clin Infect Dis 48:328-37.

3. Luo Z, Li Z, Martin L, Wan Z, Meissner EG, Espinosa E, Wu H, Yu X, Fu P, Julia Westerink MA, Kilby JM, Wu J, Huang L, Heath SL, Li Z, Jiang W. 2017. Pathological Role of Anti-CD4 Antibodies in HIV-Infected Immunologic Nonresponders Receiving Virus-Suppressive Antiretroviral Therapy. J Infect Dis 216:82-91.

4. Lisco A, Wong CS, Lage SL, Levy I, Brophy J, Lennox J, Manion M, Anderson MV, Mejia Y, Grivas C, Mystakelis H, Burbelo PD, Perez-Diez A, Rupert A, Martens CA, Anzick SL, Morse C, Chan S, Deleage C, Sereti I. 2019. Identification of rare HIV-1-infected patients with extreme CD4+ T cell decline despite ART-mediated viral suppression. JCI Insight 4.

5. Bowler SA, Premeaux TA, Ratzan L, Friday C, Gianella S, Landay AL, Ndhlovu LC, NWCS ACTG. 2025. Plasma anti-CD4 IgG levels are associated with poor immune recovery in people with HIV initiating antiretroviral therapy. AIDS 39:208-210.

6. Ning W, Cheng D, Howe PH, Bian C, Kamen DL, Luo Z, Fu X, Ogunrinde E, Yang L, Wang X, Li QZ, Oates J, Zhang W, White D, Wan Z, Gilkeson GS, Jiang W. 2022. Staphylococcus aureus peptidoglycan (PGN) induces pathogenic autoantibody production via autoreactive B cell receptor clonal selection, implications in systemic lupus erythematosus. J Autoimmun 131:102860.

7. Luo Z, Li M, Wu Y, Meng Z, Martin L, Zhang L, Ogunrinde E, Zhou Z, Qin S, Wan Z, Westerink MAJ, Warth S, Liu H, Jin P, Stroncek D, Li QZ, Wang E, Wu X, Heath SL, Li Z, Alekseyenko AV, Jiang W. 2019. Systemic translocation of Staphylococcus drives autoantibody production in HIV disease. Microbiome 7:25.

8. Wolf AJ, Underhill DM. 2018. Peptidoglycan recognition by the innate immune system. Nat Rev Immunol 18:243-254.

9. Rossetti B, Lombardi F, Belmonti S, D'Andrea MM, Tordini G, D'Avino A, Borghetti A, Moschese D, De Luca A, Montagnani F. 2019. Nasopharingeal bacterial and fungal colonization in HIV-positive versus HIV-negative adults. New Microbiol 42:37-42.

10. Song A, Li Z, Luo Z, Lu X, Wang R, Liu L, Xia W, Wan Z, Zhang T, Su B, Jiang W, Wu H. 2020. Effects of Early and Delayed Antiretroviral Therapy on Plasma Anti-CD4 Autoreactive IgG and Its Association With CD4(+) T-Cell Recovery in Acute HIV-Infected Individuals. Front Pharmacol 11:449.

11. de Taeye SW, Bentlage AEH, Mebius MM, Meesters JI, Lissenberg-Thunnissen S, Falck D, Senard T, Salehi N, Wuhrer M, Schuurman J, Labrijn AF, Rispens T, Vidarsson G. 2020. FcgammaR Binding and ADCC Activity of Human IgG Allotypes. Front Immunol 11:740.

12. Rozsnyay Z, Sarmay G, Walker M, Maslanka K, Valasek Z, Jefferis R, Gergely J. 1989. Distinctive role of IgG1 and IgG3 isotypes in Fc gamma R-mediated functions. Immunology 66:491-8.

13. Kipps TJ, Parham P, Punt J, Herzenberg LA. 1985. Importance of immunoglobulin isotype in human antibody-dependent, cell-mediated cytotoxicity directed by murine monoclonal

antibodies. J Exp Med 161:1-17.

14. Piewngam P, Khongthong S, Roekngam N, Theapparat Y, Sunpaweravong S, Faroongsarng D, Otto M. 2023. Probiotic for pathogen-specific Staphylococcus aureus decolonisation in Thailand: a phase 2, double-blind, randomised, placebo-controlled trial. Lancet Microbe 4:e75-e83.

15. Ouyang Y, Wu K, Fu L, Yi P, Cheng D, Fu X. 2025. Effect of anti-CD4 mAb induced by inhibiting B cell disorder on immune reconstruction of HIV-infected immunological non-responders. Mol Med 31:244.

16. Epling BP, Lisco A, Manion M, Laidlaw E, Galindo F, Anderson M, Roby G, Sheikh V, Migueles SA, Poole A, Perez-Diez A, Liu X, Rao VK, Burbelo PD, Sereti I. 2024. Impact of Anti-CD4 Autoantibodies on Immune Reconstitution in People With Advanced Human Immunodeficiency Virus. Clin Infect Dis doi:10.1093/cid/ciae562.

17. Lawn SD, Myer L, Bekker LG, Wood R. 2006. CD4 cell count recovery among HIV-infected patients with very advanced immunodeficiency commencing antiretroviral treatment in sub-Saharan Africa. BMC Infect Dis 6:59.

18. Chams V, Idziorek T, Klatzmann D. 1991. Biological properties of anti-CD4 autoantibodies purified from HIV-infected patients. AIDS 5:565-9.

19. Hunziker L, Recher M, Macpherson AJ, Ciurea A, Freigang S, Hengartner H, Zinkernagel RM. 2003. Hypergammaglobulinemia and autoantibody induction mechanisms in viral infections. Nat Immunol 4:343-9.

20. Zandman-Goddard G, Shoenfeld Y. 2002. HIV and autoimmunity. Autoimmun Rev 1:329-37.

21. Cheng D, Luo Z, Fitting S, Stoops W, Heath SL, Ndhlovu LC, Jiang W. 2023. The link between chronic cocaine use, B cell perturbations, and blunted immune recovery in HIV-infected individuals on suppressive ART. NeuroImmune Pharm Ther 2:71-79.

22. Olalekan AO, Schaumburg F, Nurjadi D, Dike AE, Ojurongbe O, Kolawole DO, Kun JF, Zanger P. 2012. Clonal expansion accounts for an excess of antimicrobial resistance in Staphylococcus aureus colonising HIV-positive individuals in Lagos, Nigeria. Int J Antimicrob Agents 40:268-72.

23. Loizou S, Singh S, Wypkema E, Asherson RA. 2003. Anticardiolipin, anti-beta(2)-glycoprotein I and antiprothrombin antibodies in black South African patients with infectious disease. Ann Rheum Dis 62:1106-11.

24. Becker AC, Libhaber E, Sliwa K, Singh S, Stewart S, Tikly M, Essop MR. 2011. Antiphospholipid antibodies in black south africans with hiv and acute coronary syndromes: prevalence and clinical correlates. BMC Res Notes 4:379.

25. Luo Z, Zhou Z, Ogunrinde E, Zhang T, Li Z, Martin L, Wan Z, Wu H, Qin Z, Ou T, Zhang J, Ma L, Liao G, Heath S, Huang L, Jiang W. 2017. The effect of plasma auto-IgGs on CD4+ T cell apoptosis and recovery in HIV-infected patients under antiretroviral therapy. J Leukoc Biol doi:10.1189/jlb.5A0617-219R.

26. Ramratnam B, Ribeiro R, He T, Chung C, Simon V, Vanderhoeven J, Hurley A, Zhang L, Perelson AS, Ho DD, Markowitz M. 2004. Intensification of antiretroviral therapy accelerates the decay of the HIV-1 latent reservoir and decreases, but does not eliminate, ongoing virus replication. J Acquir Immune Defic Syndr 35:33-7.

27. Veazey RS. 2019. Intestinal CD4 Depletion in HIV / SIV Infection. Curr Immunol Rev 15:76-91.

28. Danforth JM, Strieter RM, Kunkel SL, Arenberg DA, VanOtteren GM, Standiford TJ. 1995. Macrophage inflammatory protein-1 alpha expression in vivo and in vitro: the role of lipoteichoic acid. Clin Immunol Immunopathol 74:77-83.

29. Bekeredjian-Ding I, Jego G. 2009. Toll-like receptors--sentries in the B-cell response. Immunology 128:311-23.

30. Braun N, Erley C, Klein R, Kotter I, Saal J, Risler T. 2000. Immunoadsorption onto protein A induces remission in severe systemic lupus erythematosus. Nephrol Dial Transplant 15:1367-72.

31. Kim C, Siminovitch KA, Ochi A. 1991. Reduction of lupus nephritis in MRL/lpr mice by a bacterial superantigen treatment. J Exp Med 174:1431-7.

32. Williams RE. 1963. Healthy carriage of Staphylococcus aureus: its prevalence and importance. Bacteriol Rev 27:56-71.

33. Yin C, Zhang T, Qu X, Zhang Y, Putatunda R, Xiao X, Li F, Xiao W, Zhao H, Dai S, Qin X, Mo X, Young WB, Khalili K, Hu W. 2017. In Vivo Excision of HIV-1 Provirus by saCas9 and Multiplex Single-Guide RNAs in Animal Models. Mol Ther 25:1168-1186.

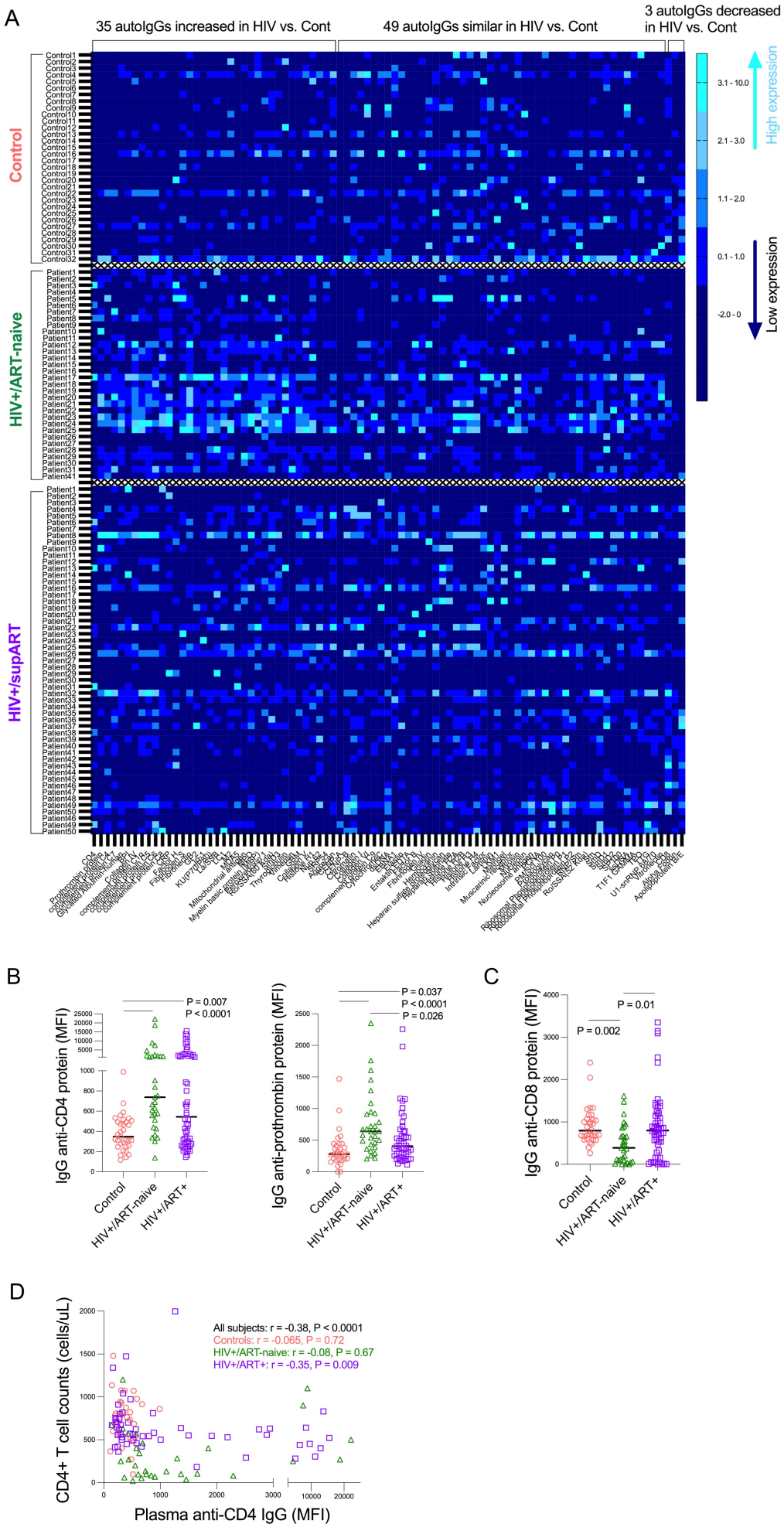
A
35 autoIgGs increased in HIV vs. Cont
49 autoIgGs similar in HIV vs. Cont
3 autoIgGs decreased in HIV vs. Cont
Control
HIV+/ART-naive
HIV+/supART
High expression
Low expression
3.1 - 10.0
2.1 - 3.0
1.1 - 2.0
0.1 - 1.0
-2.0 - 0
B
IgG anti-CD4 protein (MFI)
P = 0.007
P < 0.0001
Control
HIV+/ART-naive
HIV+/ART+
IgG anti-prothrombin protein (MFI)
P = 0.037
P < 0.0001
P = 0.026
C
IgG anti-CD8 protein (MFI)
P = 0.01
P = 0.002
D
CD4+ T cell counts (cells/uL)
Plasma anti-CD4 IgG (MFI)
All subjects: r = -0.38, P < 0.0001
Controls: r = -0.065, P = 0.72
HIV+/ART-naive: r = -0.08, P = 0.67
HIV+/ART+: r = -0.35, P = 0.009

Figure 1

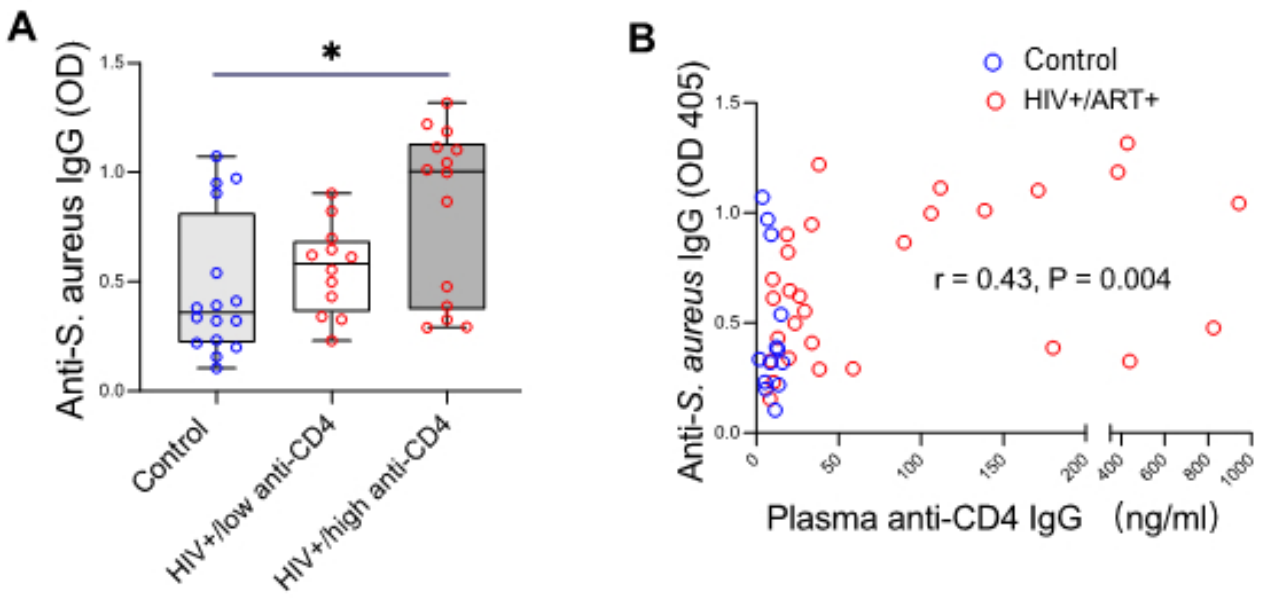
A
Anti-S. aureus IgG (OD)
1.5
1.0
0.5
0.0
*
Control
HIV+/low anti-CD4
HIV+/high anti-CD4
B
Control
HIV+/ART+
Anti-S. aureus IgG (OD 405)
r = 0.43, P = 0.004
0
50
100
150
200
400
600
800
1000
Plasma anti-CD4 IgG (ng/ml)

Figure 2

A

In vivo study

Day 1-5

i.p. EcoHIV

Day 8-100

Blood collections

Day ~100

Day 7

Antibiotics

i.p. PGN (twice/week)

Monthly

Blood collection Organ harvesting

Gut lymph nodes
Blood
Spleen

- Serum anti-CD4 & total IgG (Fig3)
- %CD4+ in CD3 (Fig 3)
- IgG binding on CD4+ (Fig 4)
- Annexin V+ on IgG+ vs IgG−; on CD4+CD3+ or CD4−CD3+ (Fig 4 &S3)

In vitro study

- Class switch DNA recombination (CSR) using splenic cells from untreated mice (Fig 5 & S6)
- %CD4+ and CD4+ apoptosis to PGN using gut lymph node cells from untreated mice (Fig S4)

B

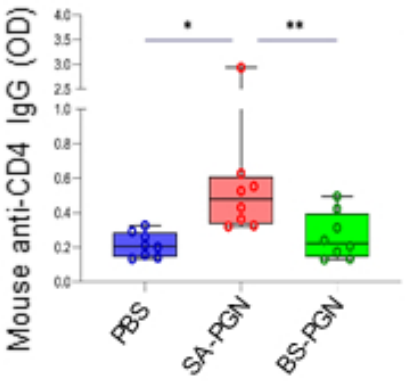

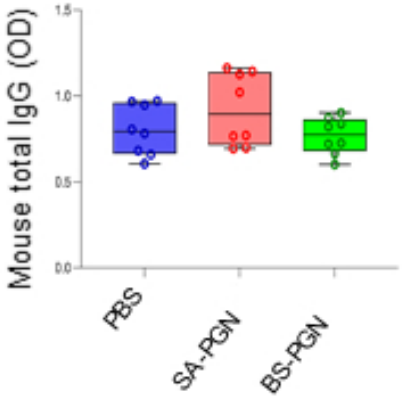

C

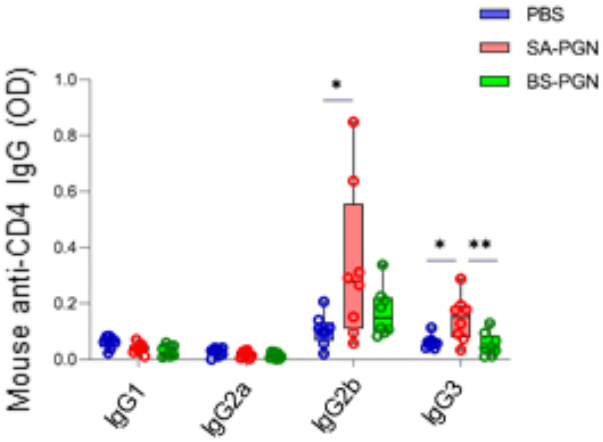

D

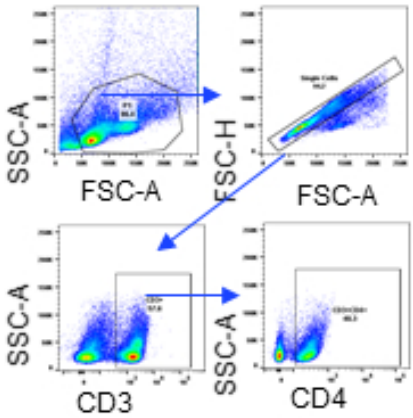

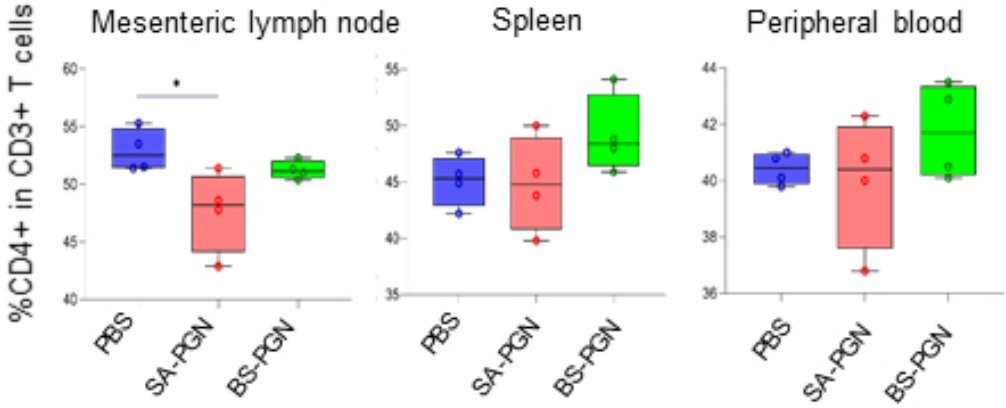

Figure 3

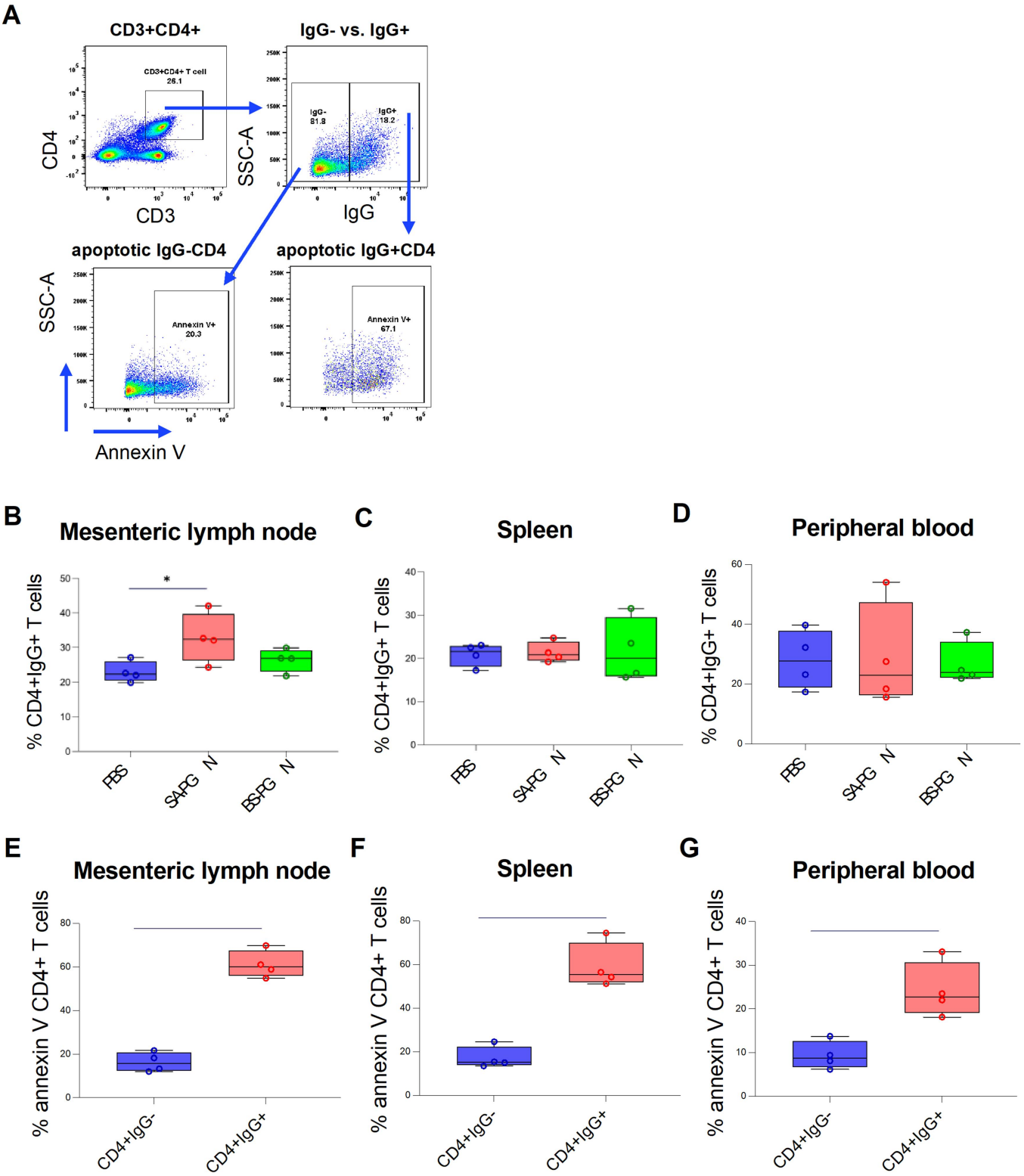
A
CD3+CD4+
IgG- vs. IgG+
CD3+CD4+ T cell
25.1
CD4
CD3
IgG-
81.8
IgG+
18.2
SSC-A
IgG
apoptotic IgG-CD4
apoptotic IgG+CD4
Annexin V+
20.3
Annexin V+
67.1
SSC-A
Annexin V
B
Mesenteric lymph node
% CD4+IgG+ T cells
FBS
SAPG N
BSPG N
C
Spleen
D
Peripheral blood
E
Mesenteric lymph node
% annexin V CD4+ T cells
CD4+IgG-
CD4+IgG+
F
Spleen
G
Peripheral blood

Figure 4

A

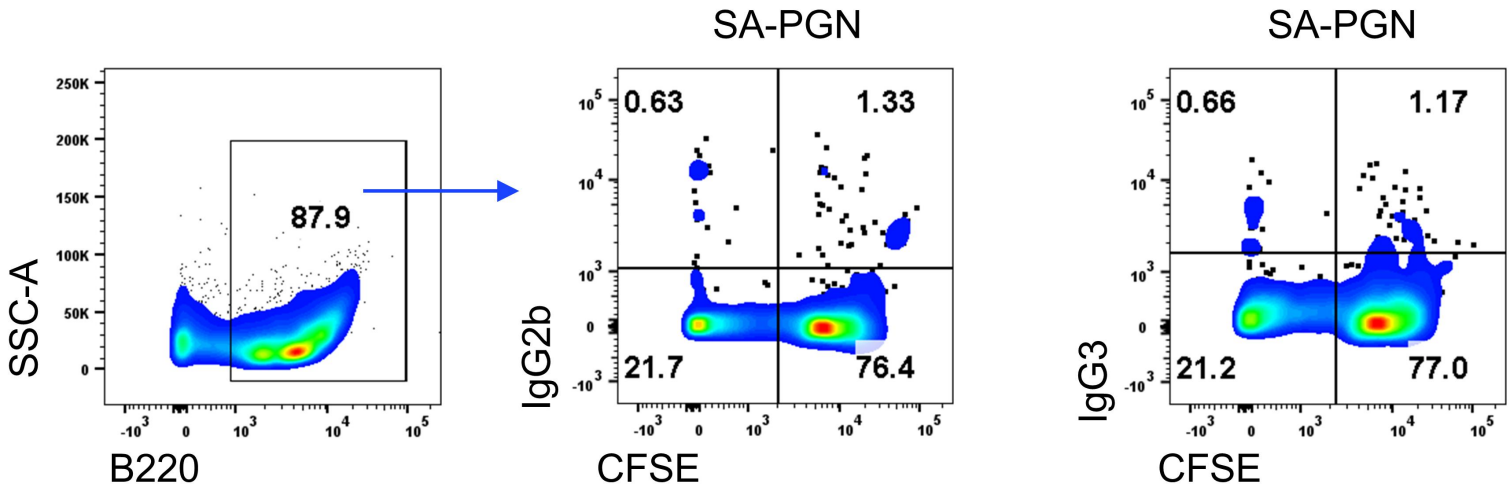
SA-PGN
SA-PGN
SSC-A
B220
87.9
IgG2b
CFSE
0.63
1.33
21.7
76.4
IgG3
CFSE
0.66
1.17
21.2
77.0

B

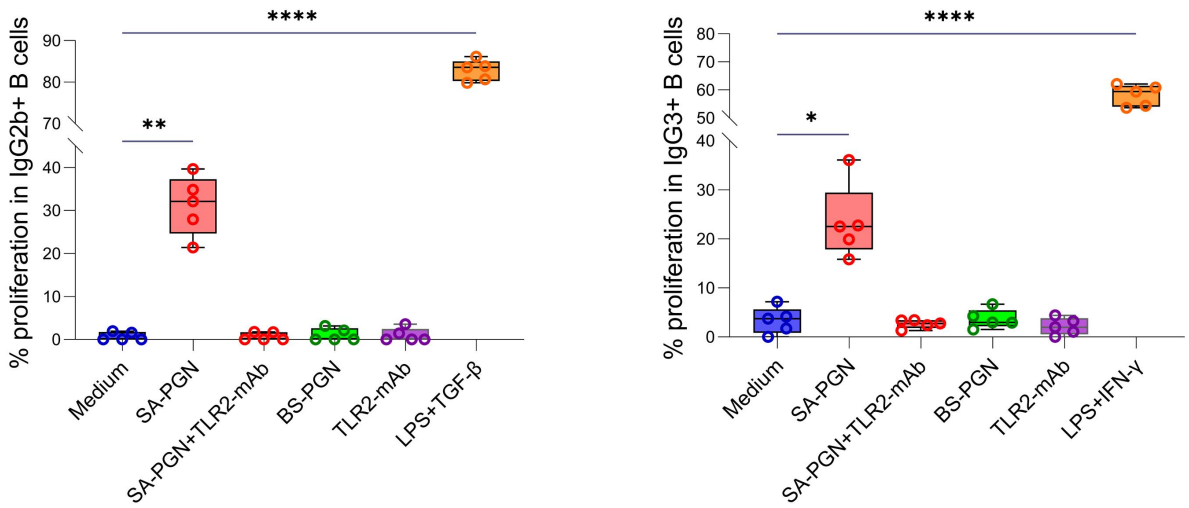
% proliferation in IgG2b+ B cells
****
**
Medium
SA-PGN
SA-PGN+TLR2-mAb
BS-PGN
TLR2-mAb
LPS+TGF-β
% proliferation in IgG3+ B cells
****
*
Medium
SA-PGN
SA-PGN+TLR2-mAb
BS-PGN
TLR2-mAb
LPS+IFN-γ

Figure 5

A

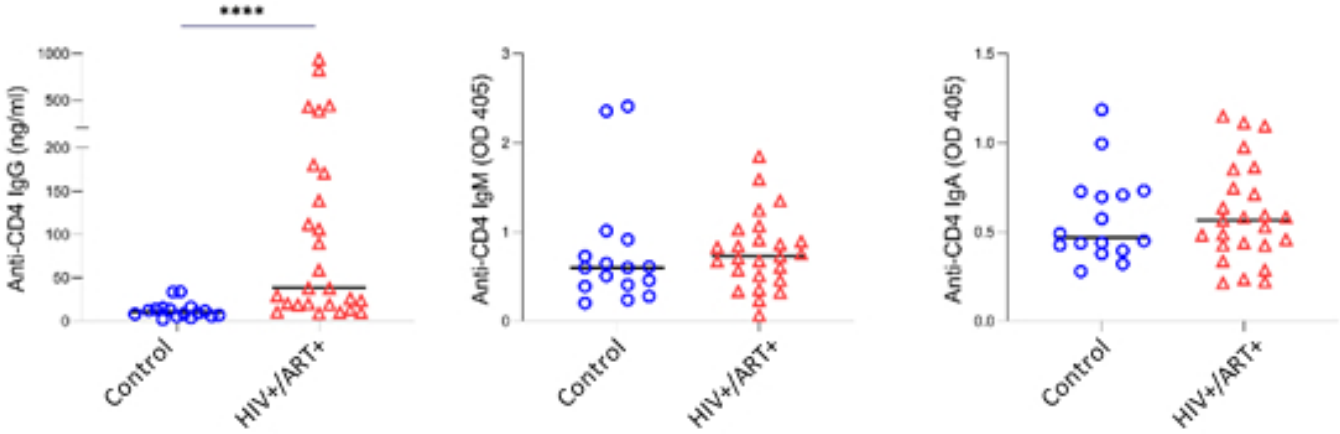
****
Anti-CD4 IgG (ng/ml)
1000
500
200
150
100
50
0
Control
HIV+/ART+
Anti-CD4 IgM (OD 405)
3
2
1
0
Control
HIV+/ART+
Anti-CD4 IgA (OD 405)
1.5
1.0
0.5
0.0
Control
HIV+/ART+

B

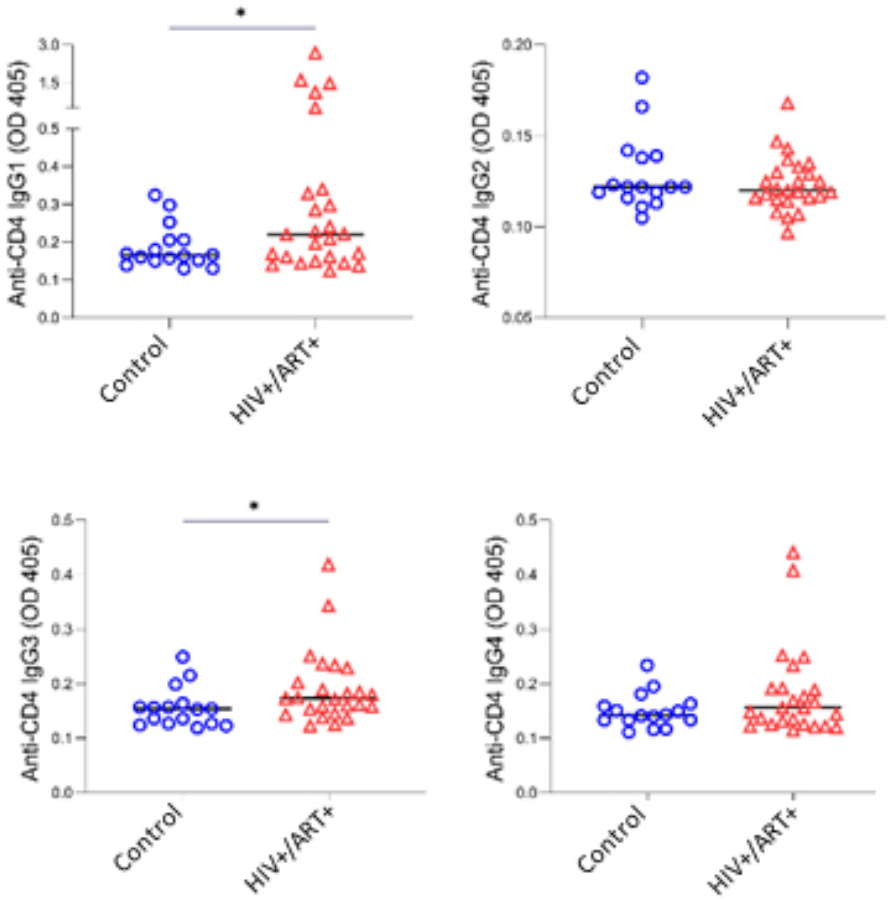
*
Anti-CD4 IgG1 (OD 405)
3.0
1.5
0.5
0.4
0.3
0.2
0.1
0.0
Control
HIV+/ART+
Anti-CD4 IgG2 (OD 405)
0.20
0.15
0.10
0.05
Control
HIV+/ART+
*
Anti-CD4 IgG3 (OD 405)
0.5
0.4
0.3
0.2
0.1
0.0
Control
HIV+/ART+
Anti-CD4 IgG4 (OD 405)
0.5
0.4
0.3
0.2
0.1
0.0
Control
HIV+/ART+

Figure S1

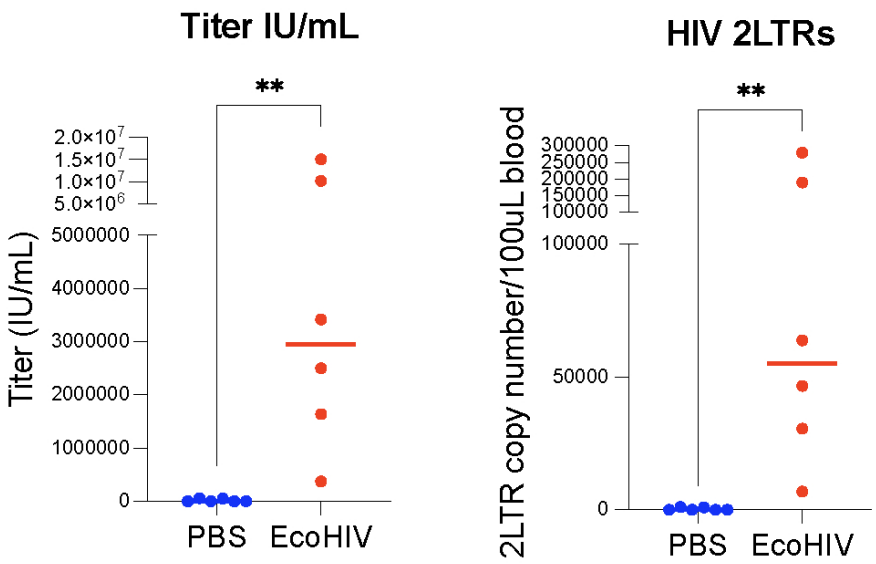
Titer IU/mL
**
2.0×10^7
1.5×10^7
1.0×10^7
5.0×10^6
5000000
4000000
3000000
2000000
1000000
0
Titer (IU/mL)
PBS
EcoHIV
HIV 2LTRs
**
300000
250000
200000
150000
100000
100000
50000
0
2LTR copy number/100uL blood
PBS
EcoHIV

Figure S2

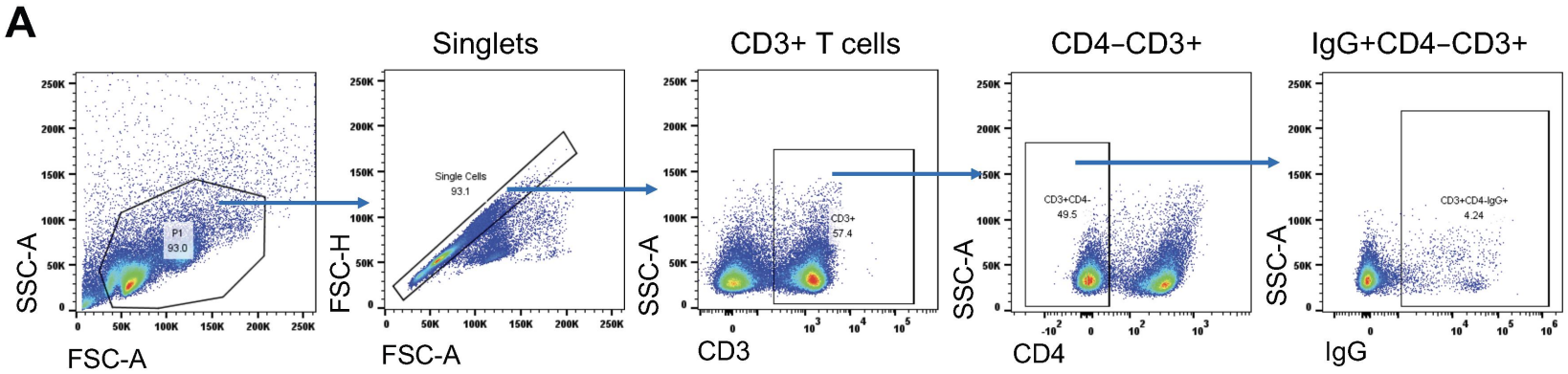
A
Singlets
CD3+ T cells
CD4−CD3+
IgG+CD4−CD3+
SSC-A
FSC-A
P1
93.0
FSC-H
Single Cells
93.1
CD3+
57.4
CD3
CD3+CD4-
49.5
CD4
CD3+CD4-IgG+
4.24
IgG

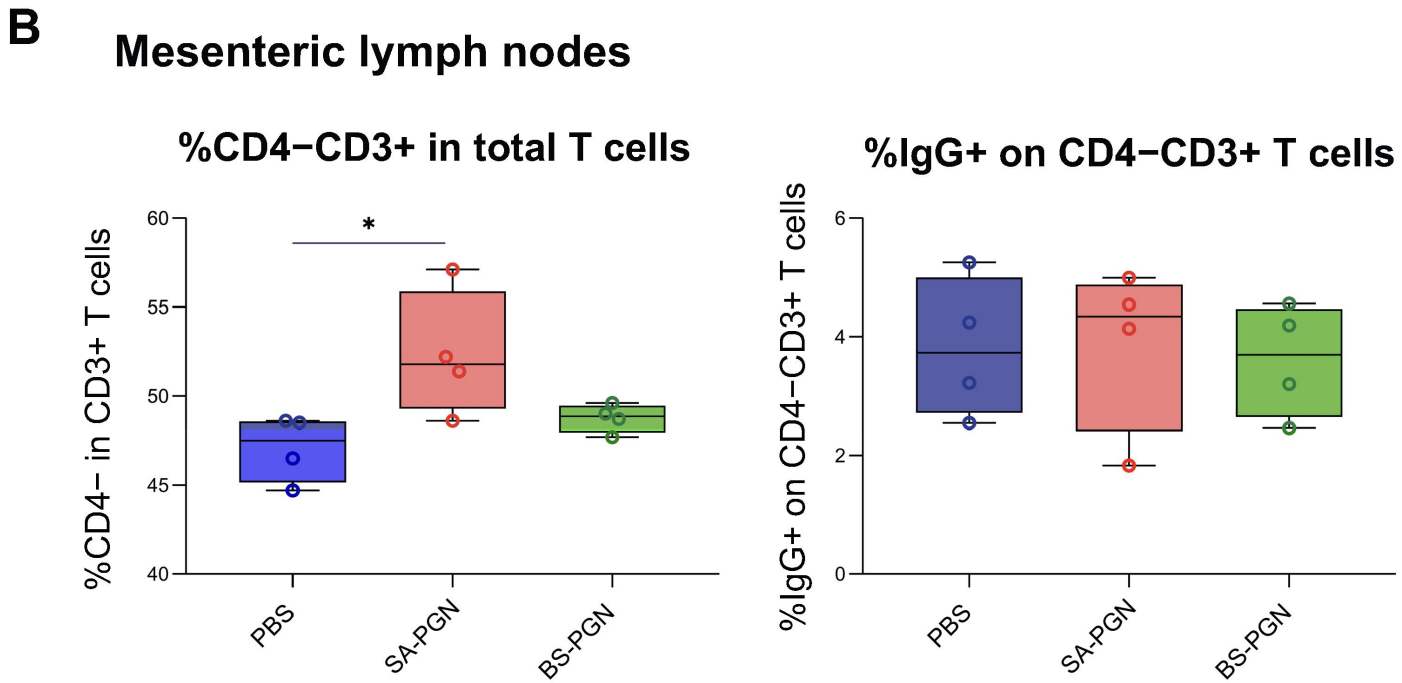
B
Mesenteric lymph nodes
%CD4−CD3+ in total T cells
%CD4− in CD3+ T cells
*
PBS
SA-PGN
BS-PGN
%IgG+ on CD4−CD3+ T cells
%IgG+ on CD4−CD3+ T cells

Figure S3

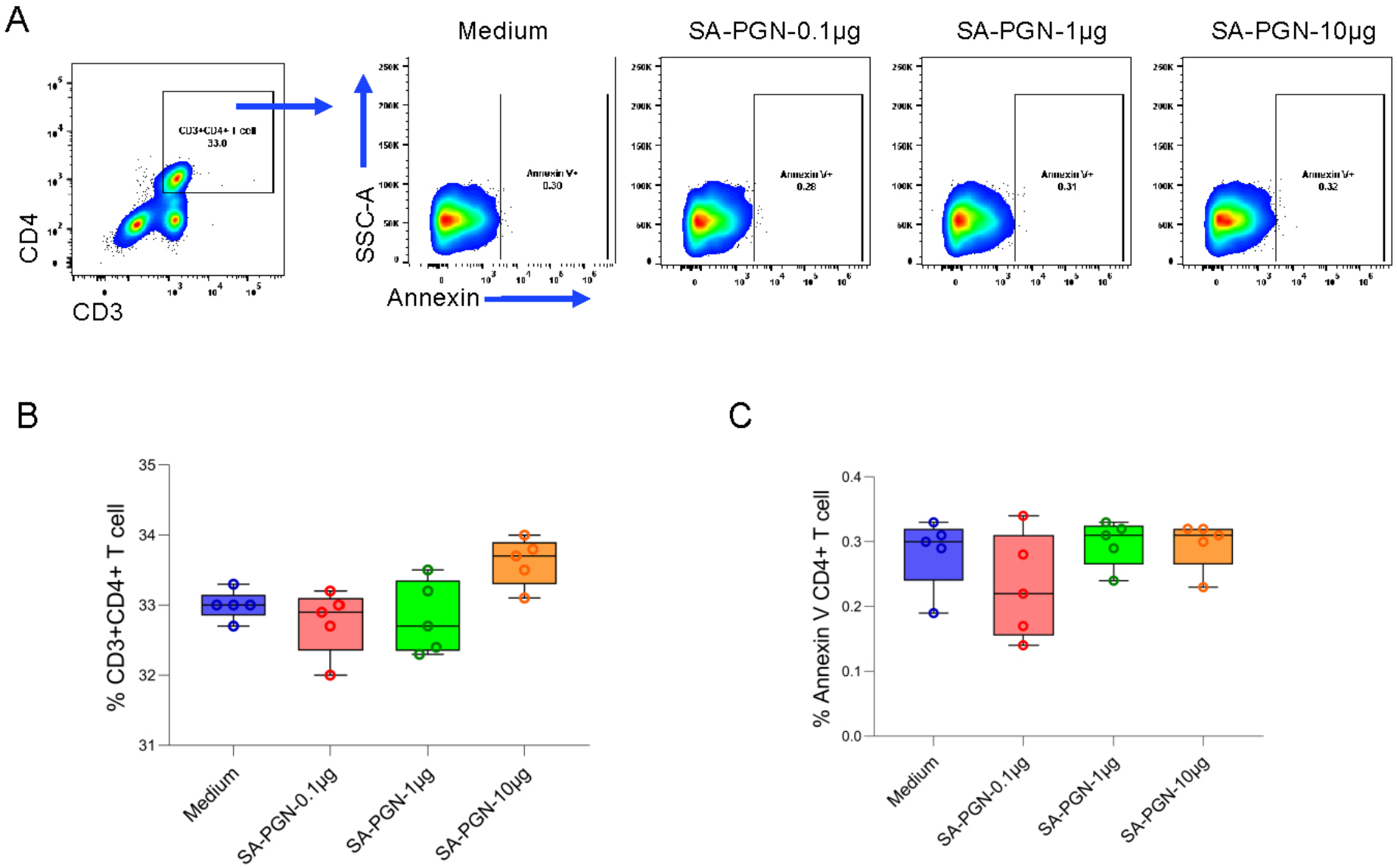
A
Medium
SA-PGN-0.1μg
SA-PGN-1μg
SA-PGN-10μg
CD4
CD3
CD3+CD4+ T cell
33.0
SSC-A
Annexin
Annexin V+
0.30
0.28
0.31
0.32
B
% CD3+CD4+ T cell
35
34
33
32
31
Medium
SA-PGN-0.1μg
SA-PGN-1μg
SA-PGN-10μg
C
% Annexin V CD4+ T cell
0.4
0.3
0.2
0.1
0.0
Medium
SA-PGN-0.1μg
SA-PGN-1μg
SA-PGN-10μg

Figure S4

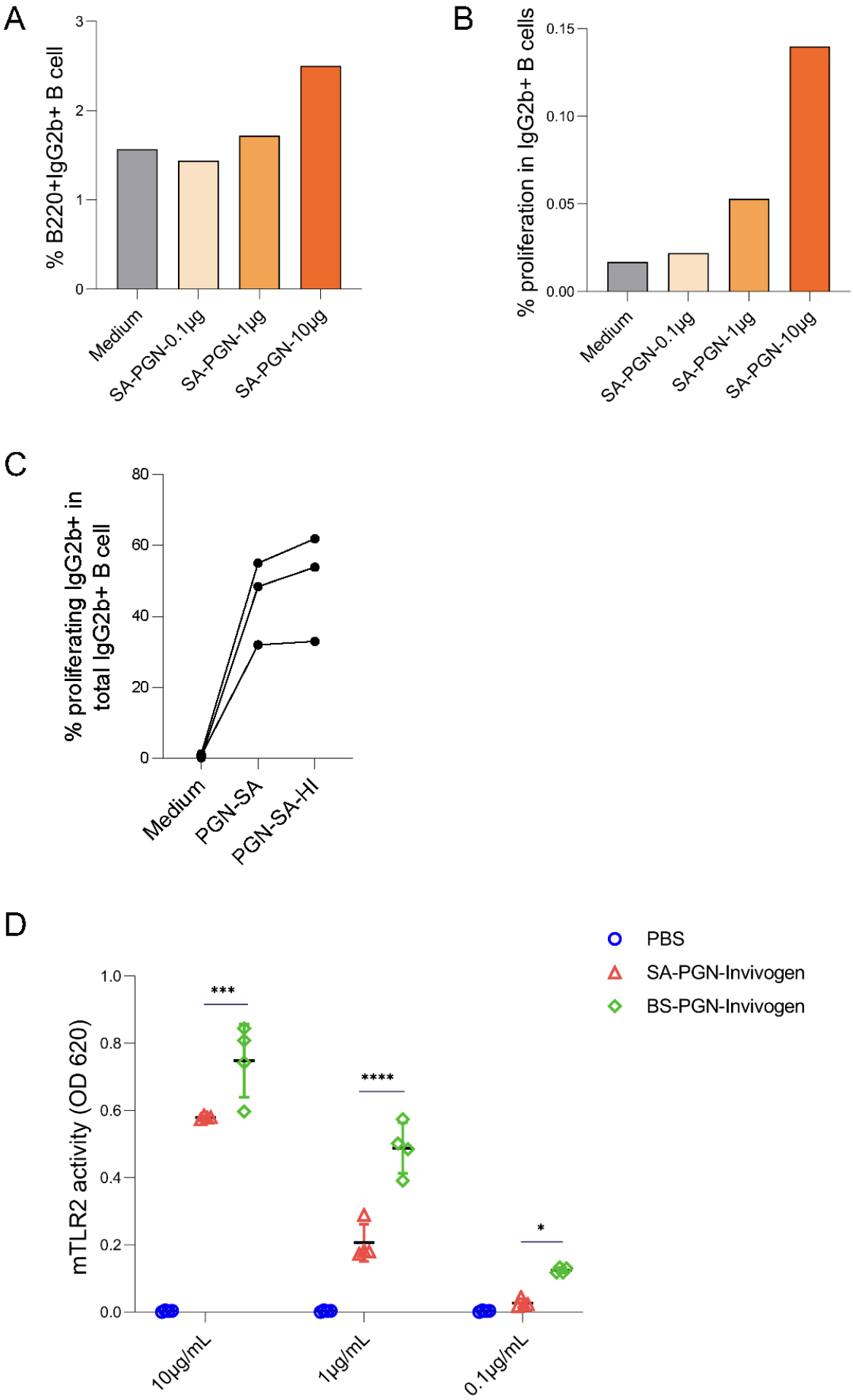
A
% B220+IgG2b+ B cell
3
2
1
0
Medium
SA-PGN-0.1μg
SA-PGN-1μg
SA-PGN-10μg
B
% proliferation in IgG2b+ B cells
0.15
0.10
0.05
0.00
Medium
SA-PGN-0.1μg
SA-PGN-1μg
SA-PGN-10μg
C
% proliferating IgG2b+ in total IgG2b+ B cell
80
60
40
20
0
Medium
PGN-SA
PGN-SA-HI
D
PBS
SA-PGN-Invivogen
BS-PGN-Invivogen
mTLR2 activity (OD 620)
1.0
0.8
0.6
0.4
0.2
0.0
***
****
*
10μg/mL
1μg/mL
0.1μg/mL

Figure S5

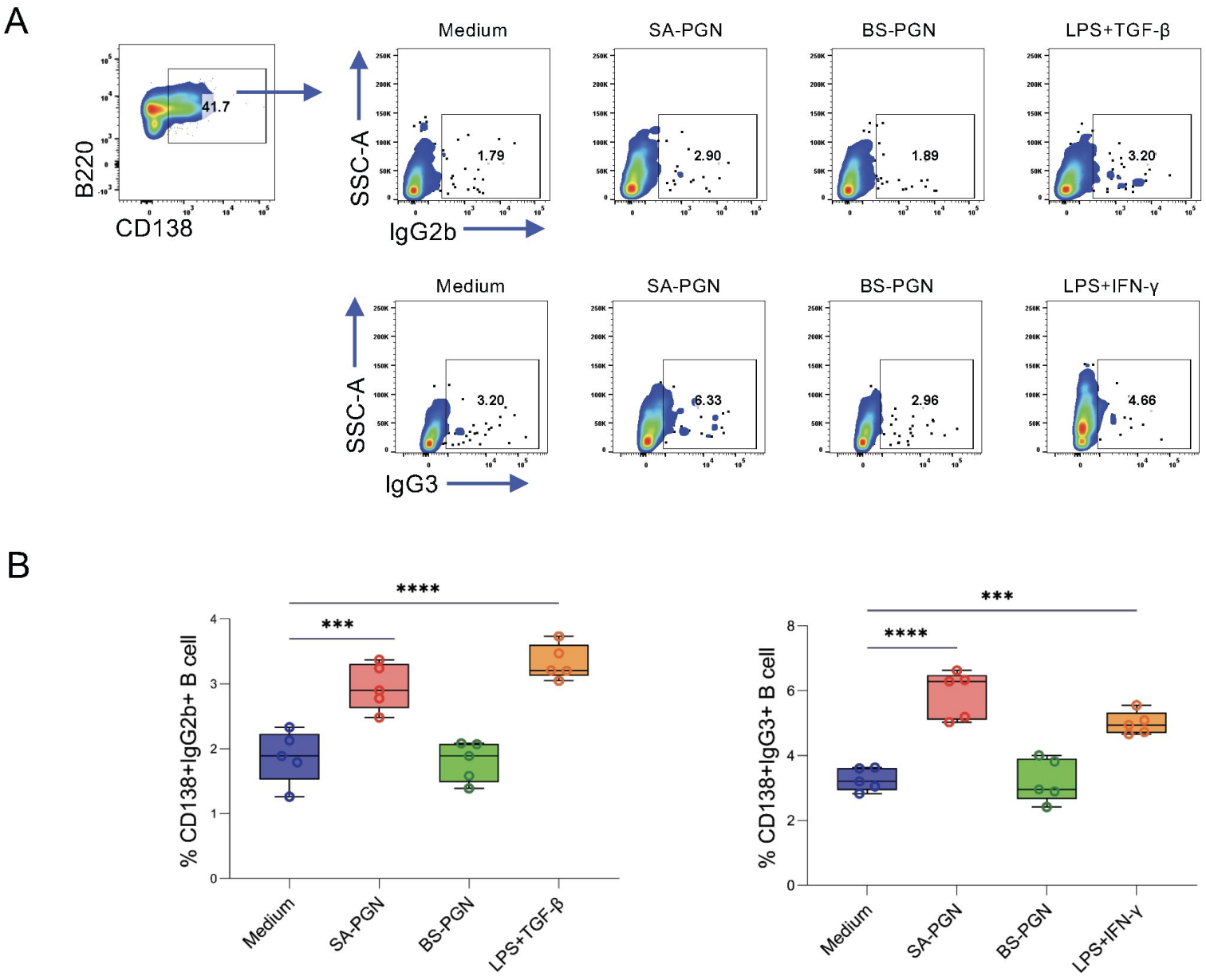
A
B220
CD138
41.7
Medium
SA-PGN
BS-PGN
LPS+TGF-β
SSC-A
IgG2b
1.79
2.90
1.89
3.20
LPS+IFN-γ
IgG3
3.20
6.33
2.96
4.66
B
% CD138+IgG2b+ B cell
% CD138+IgG3+ B cell
****
***

Figure S6